Journal of Medicinal Chemistry

ARTICLE

pubs.acs.org/jmc

Structure-Based Discovery of Inhibitors of Microsomal Prostaglandin E_2 Synthase−1, 5-Lipoxygenase and 5-Lipoxygenase-Activating Protein: Promising Hits for the Development of New Anti-inflammatory Agents

Rosa De Simone,[†] Maria Giovanna Chini,[†] Ines Bruno,[*,†] Raffaele Riccio,[†] Daniela Mueller,[‡] Oliver Werz,[‡] and Giuseppe Bifulco[*,†]

[†]Department of Pharmaceutical Sciences, University of Salerno, Via Ponte Don Melillo, 84084 Fisciano (SA), Italy

[‡]Department of Pharmaceutical Analytics, Pharmaceutical Institute, University of Tuebingen, Auf der Morgenstelle 8, D-72076 Tuebingen, Germany

Supporting Information

ABSTRACT: Microsomal prostaglandin E_2 synthase (mPGES)-1 catalyzes the transformation of PGH_2 to PGE_2 that is involved in several pathologies like fever, pain, and inflammatory disorders. To identify novel mPGES-1 inhibitors, we used in silico screening to rapidly direct the synthesis, based on the copper-catalyzed 3 + 2 Huisgen's reaction (click chemistry), of potential inhibitors. We designed 26 new triazole-based compounds in accordance with the pocket binding requirements of human mPGES-1. Docking results, in agreement with ligand efficiency values, suggested the synthesis of 15 compounds that at least in theory were shown to be more efficient in inhibiting mPGES-1. Biological evaluation of these selected compounds has disclosed three new potential anti-inflammatory drugs: (I) compound **4** displaying selectivity for mPGES-1 with an IC_{50} value of 3.2 μM, (II) compound **20** that dually inhibits 5-lipoxygenase and mPGES-1, and (III) compound **7** apparently acting as 5-lipoxygenase-activating protein inhibitor (IC_{50} = 0.4 μM).

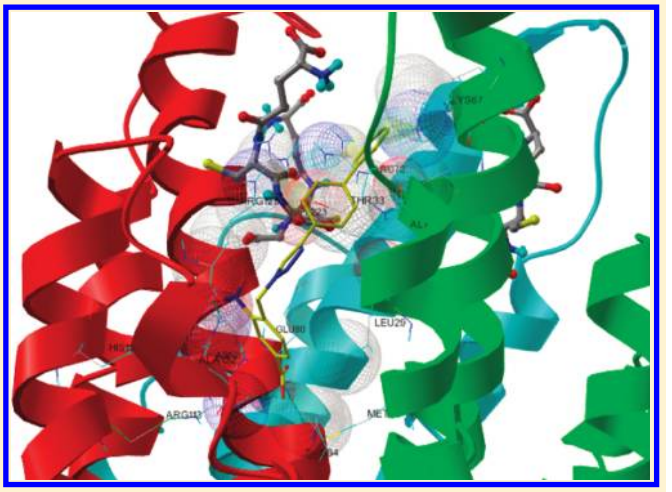

INTRODUCTION

Nonsteroidal anti-inflammatory drugs (NSAIDs) represent so far the pivot of inflammation therapy as a consequence of their potent effect in the suppression of prostaglandins (PGs), prominent bioactive mediators involved in key physiological functions[1] and also implicated in several pathologic conditions like inflammation and tumorigenesis.[2] However, especially for long-term treatments—like those required for chronic pathologies such as rheumatoid arthritis—their use comprises severe side effects; in particular, NSAIDs are well-known to be endowed with relevant gastric toxicity[3] due to the efficient suppression of constitutively generated PGE_2 involving the cyclooxygenase (COX)-1 pathway with gastro-protection functions. Not long ago, the introduction of coxibs in therapy was initially considered as a solution of all of the problems connected with the use of NSAIDs, as these selective COX-2 inhibitors were shown to exhibit potent anti-inflammatory activity without causing significant gastrointestinal injury. Unfortunately, various clinical evidence indicated their implication in serious cardiovascular accidents.[4] In this perspective, there is an ever growing need for the research of safer anti-inflammatory drugs.

Recently, great attention has been focused on the microsomal prostaglandin E_2 synthase (mPGES)-1 enzyme responsible for the conversion of the COX-derived unstable peroxide PGH_2 into PGE_2; this enzyme is overexpressed in several inflammatory disorders[5] as well as in many human tumors.[6−8] Inhibition of microsomal prostaglandin E_2 synthase-1 (mPGES-1) has been proposed as a more promising approach for the development of safer drugs in inflammatory disorders,[9,10] devoid of classical NSAID side effects, as this inducible enzyme affects the biosynthesis of massive PGE_2 generation as a response to inflammatory stimuli.[11] mPGES-1 is a glutathione (GSH)-dependent transmembrane enzyme belonging to the MAPEG (membrane-associated proteins involved in eicosanoid and glutathione metabolism) family. This protein family consists of membrane-bound proteins, with diverse functions, like leukotriene C_4 synthase (LTCS), microsomal glutathione transferase-1 (MGST-1), and 5-lipoxygenase-activating protein (FLAP). Among the three isoforms so far identified for prostaglandin E synthase (PGES), it is mPGES-1,

Received: July 22, 2010
Published: February 16, 2011

Chart 1. Chemical Structures of Compounds 1−26 Utilized for Molecular Docking Studies

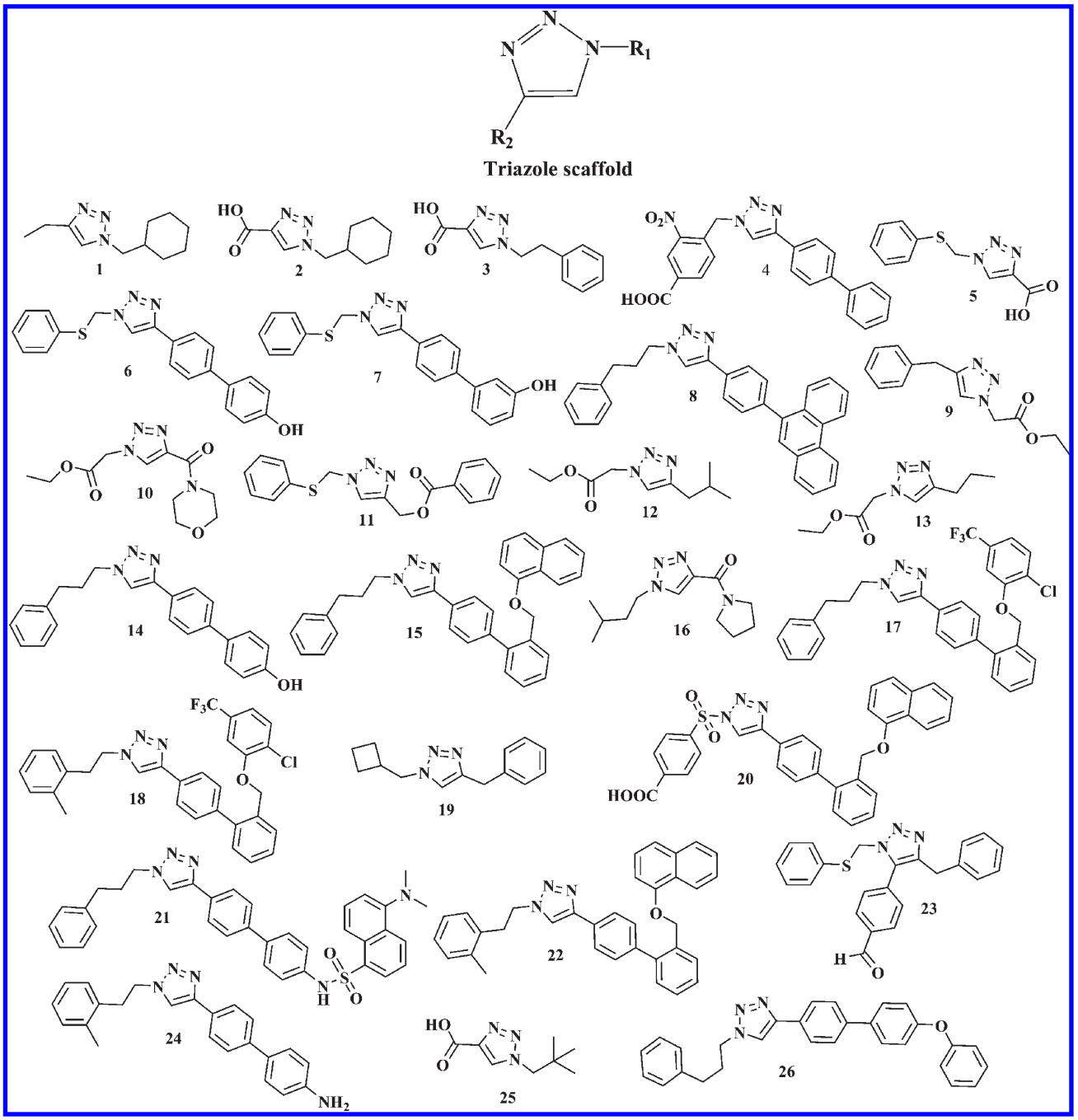

functionally coupled with COX-2, that seems to be the isoform primarily involved in pathologies.[11]

Even though Jegerschöld et al.[12] have recently elucidated the electron crystallographic structure of closed conformation of mPGES-1, the open form of the protein constitutes a model for the productive enzyme. Therefore, the absence of the three-dimensional (3D) X-ray crystal structure of the open mPGES-1 conformation with a substrate or an inhibitor bound has represented a major difficulty for the rational design of new specific inhibitors, making the classical receptor-based approach quite challenging. In fact, despite many efforts spent in this area, only very few effective in vivo mPGES-1 inhibitors have been reported in literature; therefore, the discovery of potent inhibitors of this interesting target would be of great relevance for the development of a new generation of anti-inflammatory agents with potentially safer profiles.

By means of an in silico screening, we describe here the development of fast synthetically accessible triazole-based compounds,[13−19] representing innovative scaffolds in this area as potential mPGES-1 inhibitors. In the course of our screening, we discovered a very promising dual inhibitor of mPGES-1 and 5-LO, and we identified other compounds of interest that may provide precious guidelines for the drug development process.

RESULTS AND DISCUSSION

Molecular Docking Studies. The lack of a 3D X-ray crystal structure of open mPGES-1 conformation has stimulated many efforts for identifying the key characteristics of mPGES-1 inhibitors, based on quantum mechanic (QM) calculations,[20] structure−activity relationship (SAR)[21,22] and 3D quantitative structure−activity relationship (3D-QSAR) analysis,[23−26] multistep ligand-based strategy,[27] high-throughput screening (HTS),[28] molecular modeling and dynamics simulation,[29] and site-direct mutagenesis studies.[30] As reported by Friesen et al.,[10] these efforts have led to the identification of several classes of mPGES-1 inhibitors: fatty acids and PGH_2 analogues,[31] indole and **43** (MK-886, Chart 2) analogues,[32] phenantrene imidazoles,[28] nonacidic agents,[27] and other inhibitors. Considering the well-known characteristic of indole-based agents—the simultaneous contributions to the inhibitory activity on mPGES-1 of hydrophobic and electrostatic effects—and the ring size of fatty acids and PGH_2 analogues as starting point, we designed new triazole nucleus templates as potential scaffolds for anti-inflammatory drugs. We designed a small set of compounds (Chart 1) decorating a disubstituted triazole ring, taking into account both the synthetic accessibility and the compatibility of R_1 and R_2 groups with the binding requirements of the pocket situated in the region at the interface of the two mPGES-1 subunits. In particular, we gradually increased the length, size, and hydro- and lipophilicity of R_1 and R_2 with the aim to optimize their chemophysical properties. To identify the key structural features necessary for mPGES-1 inhibition, we performed an in silico screening by molecular docking using AutoDock 3.0.5 software[33] of a small set of molecules. For our docking calculation, we used the MGST-1 structure solved by Holm et al. in 2006[34] in which significant amino acid conservation in comparison to mPGES-1[35] (38% of homology sequence) can be recognized. Recently, the structure-based drug design targeting mPGES-1 was facilitated by the work of Hamza et al.,[29,30] who have described the PGH_2 binding to the mPGES-1−GSH complex. More precisely, as also demonstrated by site direct mutagenesis, the natural ligand at the interface of

Table 1. List of the Corresponding Amino Acids Present in Both mPGES-1 and MGST-1 Catalytic Sites

mPGES-1	MGST-1
Arg110	Arg113
Arg70	Arg73
Asn74	Asn77
Tyr117	Tyr120
Leu121	Leu124
Arg126	Arg129
His72	His75
Lys26	Lys25
Glu66	Glu69
His113	His116
Arg73	Leu76
Arg122	Pro125
Thr129	Ala132
Leu69	Arg72
Ile125	Asn128
Thr78	Asn81
Tyr130	Phe133

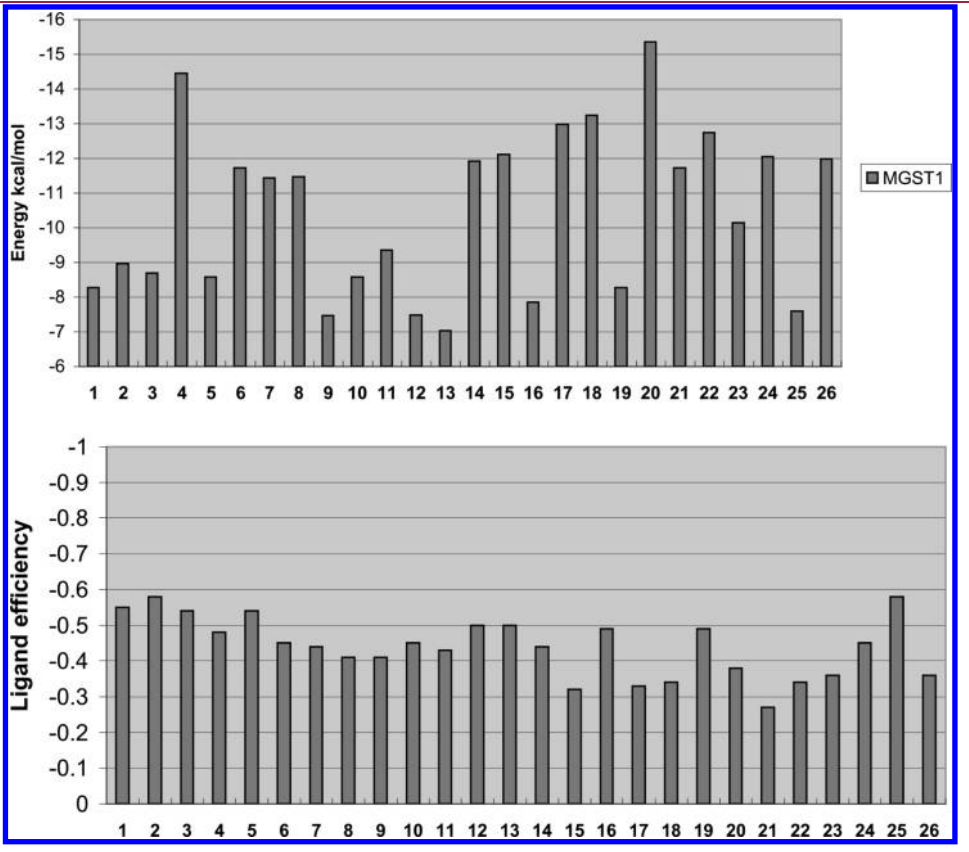

Figure 1. Calculated affinities and ligand efficiency of compounds **1**−**26** for MGST-1.

dx.doi.org/10.1021/jm101238d |*J. Med. Chem.* 2011, 54, 1565–1575

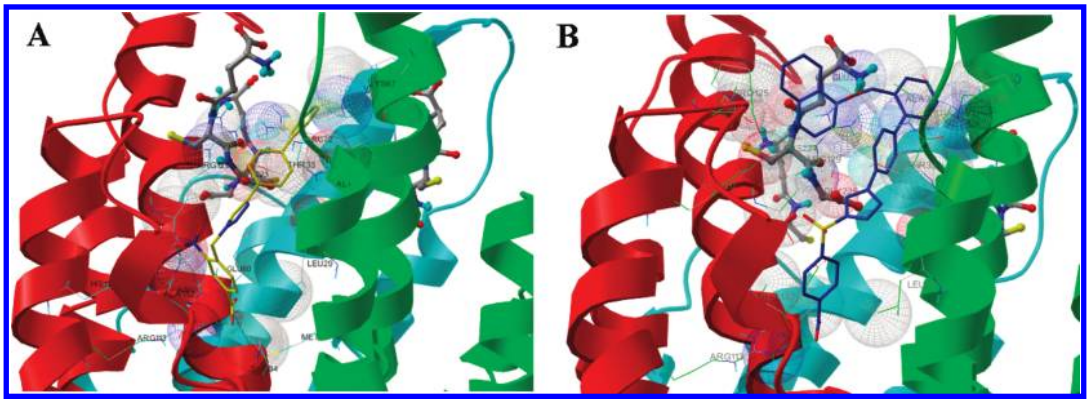

Figure 2. Three-dimensional model of interactions of **4** (A) and **20** (B) with the MGST-1 binding site. The protein is represented by secondary structure, by CPK, and by lines colored by atom type (C, gray; polar H, sky blue; N, blue; and O, red). Compound **4** (A) is depicted by sticks and balls (by atom type: C, yellow; O, red; and N, blue). Compound **20** (B) is depicted by sticks and balls (by atom type: C, blue; O, red; N, dark blue; and S, yellow).

Scheme 1. Synthetic Strategy for the Synthesis of Compounds 4, 6−8, 11, 14, 15, 17, 18, 20−22, 24, and 26[a]

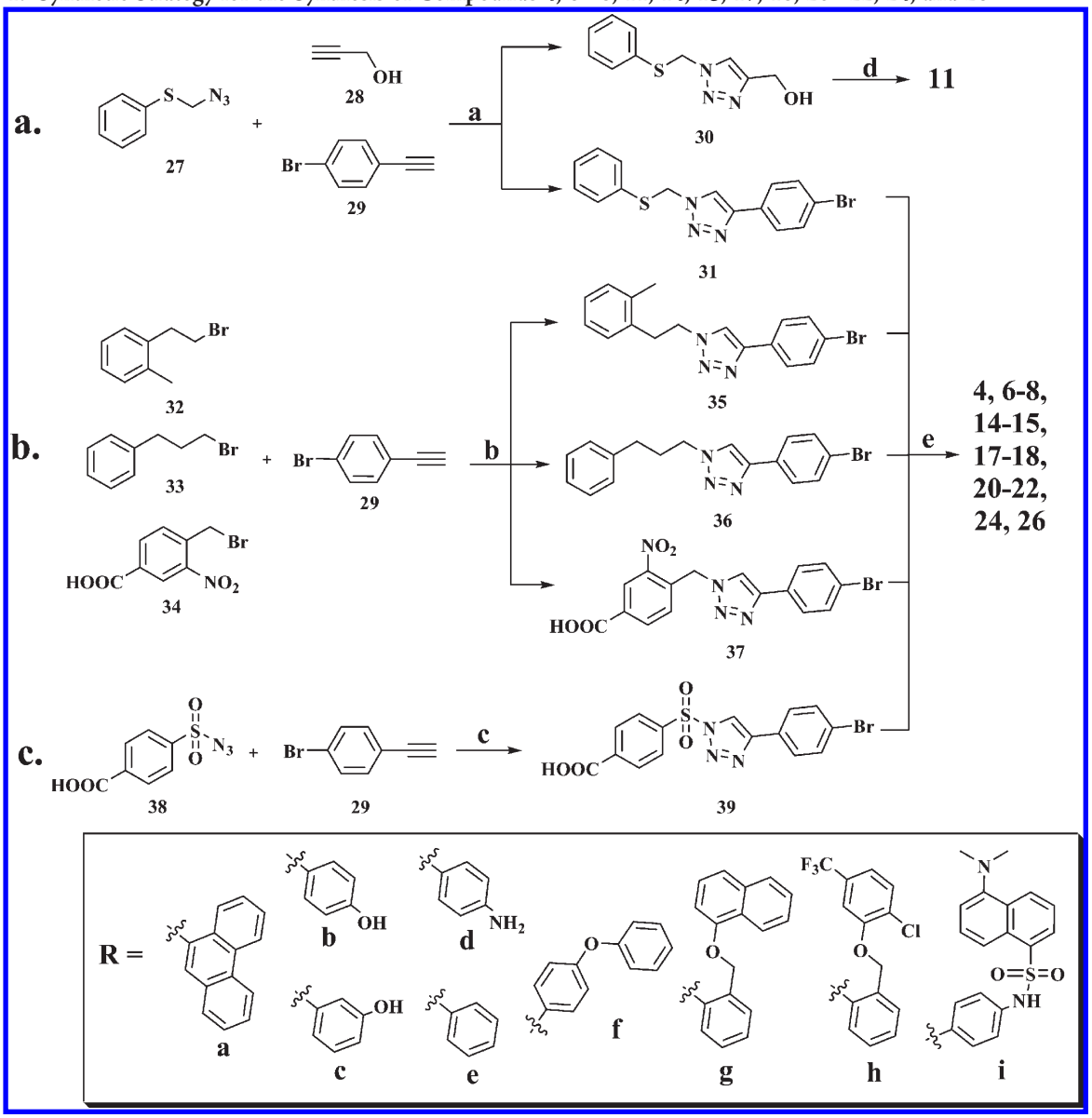

[a] Reagents and conditions: (a) $CuSO_4$, sodium ascorbate, H_2O/*t*-BuOH 1:1, room temperature, overnight. (b) $CuSO_4$, Cu(0), NaN_3, *t*-BuOH/H_2O 1:1, microwaves, 30 min. (c) CuI, 2,6-lutidine, $CHCl_3$ dry, 12 h, 0 °C. (d) C_6H_5COCl, DMF dry, reflux, overnight. (e) $RB(OH)_2$ (a−i), CsF, $Pd(dppf)Cl_2$, H_2O/THF 1:1, microwaves, 20−30 min.

dx.doi.org/10.1021/jm101238d |*J. Med. Chem.* 2011, 54, 1565–1575

Scheme 2. Synthetic Strategy for the Synthesis of Compound 23[a]

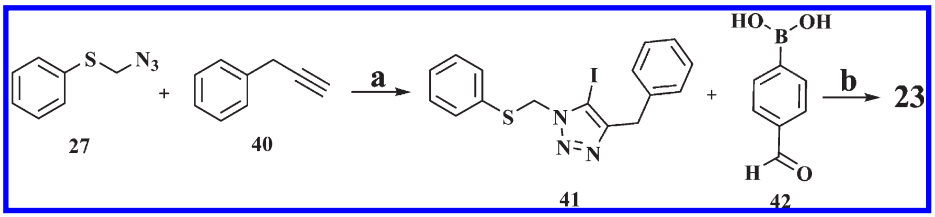

[a] Reagents and conditions: (a) CuI, DIPEA, NBS, THF, room temperature, 4 h. (b) CsF, Pd(dppf)Cl_2, H_2O/THF 1:1, microwaves, 30 min.

Table 2. Effect of Test Compounds on the Activity of mPGES-1[a]

	mPGES-1 activity	
compound	IC $_{50}$ (μM)	remaining activity at 30 μM (%)
4	3.2	12.0 ± 3.7**
6	>30	89.0 ± 2.9
7	>30	60.1 ± 4.3**
8	>30	78.2 ± 12.8
11	>30	76.1 ± 7.9
14	>30	73.6 ± 8.0
15	>30	96.8 ± 0.5
17	>30	91.9 ± 8.1
18	>30	87.9 ± 8.4
20	>30	59.8 ± 7.2**
21	>30	85.0 ± 9.3
22	>30	90.0 ± 6.8
23	>30	72.1 ± 4.2*
24	>30	98.2 ± 7.3
26	>30	88.7 ± 2.7

[a] Data are given as means ± SEs, n = 4−6. *p < 0.05, and **p < 0.01.

each mPGES-1 monomer establishes a strong salt bridge between its carboxylate group and the highly conserved Arg110 in the MAPEG family and interacts with Arg70, Asn74, Arg73, Glu77, Tyr117, Leu121, Arg122, Arg126, Thr129, Arg110, His72, Lys26, Leu69, and Ile125. Taking into account the considerations above, we referred to the sequence alignment of these two MAPEG super family members for the rationalization of the small molecules binding mode (Table 1).[29] The theoretical affinities of compounds **1**−**26** calculated by docking, reported as the most favorable MGST-1 free energy of binding together with the ligand efficiency[36−39] (binding energy for heavy atom molecular ΔG/NHA), are shown in Figure 1.

The data shown in Figure 1 indicate the best calculated affinities for compounds presenting one H-bond acceptor group and a lipophilic substituent of adequate dimensions.[39] For the sake of simplicity, we report the most promising candidates derived from the in silico screening, **4** and **20** (Figure 2), to trace the features of new potential anti-inflammatory drugs.

From the analysis of the results, both compounds disclosed a similar binding mode at the interface of the target monomer. Our proposed poses are in agreement with the model reported by Hamza et al.[29] In fact, the compounds interact with residues considered critical for PGH_2 binding, such as the hydrogen bonds with the carboxy group in **4** and **20** with the highly conserved Arg113 in MGST-1 ($Arg110_{mPGES-1}$), guaranteeing, at least in theory, the enzyme binding specificity, as well as van der Waals and other interactions with residues of the active site—the cation−π interaction with Lys67, Arg72, and Arg196 for **4** and with Lys67 and Arg196 for **20**. The above in silico results suggested the synthesis of the molecules **4**, **6**−**8**, **11**, **14**, **15**, **17**, **18**, **20**−**24**, and **26**, all within the lowest free energy of binding and a good ligand efficiency ($E_{binding}$ < 9 kcal/mol and ΔG/NHA deeper than −0.24 kcal/mol) as the starting point for obtaining preliminary experimental results. The evaluation of the bioactivity of this small set of compounds might be helpful for the comprehension of the key features of new mPGES-1 triazole-based inhibitors.

Chemistry. For the synthesis of compounds **4**, **6**−**8**, **11**, **14**, **15**, **17**, **18**, **20**−**22**, **24**, and **26**, we utilized the synthetic procedure outlined in Scheme 1. Except for **11**, we took advantage of 1,3-dipolar cycloaddition reaction (click reaction) to generate the triazole intermediates **30**, **31**, **35**−**37**, and **39** that were successively subjected to the Suzuki cross-coupling reaction with the appropriate commercially available boronic acids a−i. The triazoles intermediates were generated through the condensation between the appropriate terminal alkynes and the azides. In more detail, when we started from the commercially available azide **27**, the traditional protocol for 1,3-dipolar cycloaddition at room temperature for 18 h in the presence of $CuSO_4$ as catalyst and sodium ascorbate in a mixture of *tert*-butanol/water (*t*-BuOH/H_2O) 1:1 was used (Scheme 1a).[40] On the contrary, when the azides were generated in situ with sodium azide starting from the corresponding halides, the microwave irradiation technique provided a faster way to obtain the desired triazole intermediates **35**−**37** (Scheme 1b) in a one-pot reaction.[41]

The synthesis of intermediate **39** required a different procedure because of the presence of the sulfonyl functionality, which is a strong electron-withdrawing group that could negatively affect the reaction outcome and favor a rapid conversion of the Cu-containing transition state into a variety of byproduct rather than the desired cycloadduct.[42,43] However, we were able to obtain the desired sulfonyl triazole intermediate **39**, carrying out the cycloaddition between 1-bromo-4-ethynylbenzene **29** and 4-carboxybenzenesulfonazide **38** in dry chloroform at 0 °C in presence of 2,6-lutidine as base (Scheme 1c).[44]

The triazole intermediates **31**, **35**−**37**, and **39** were finally subjected to the Suzuki cross-coupling reaction with the appropriate boronic acids a−i following the experimental conditions previously optimized by us,[45] providing for the use of [1,1′-bis-(diphenylphosphino)ferrocene]dichloropalladium(II) (Pd(dppf)-Cl_2) as a catalyst and CsF as a base in a mixture of tetrahydrofuran/water (THF/H_2O) 1:1, under microwave irradiation; the desired final compounds **4**, **6**−**8**, **14**, **15**, **17**, **18**, **20**−**22**, **24**, and **26** (Chart 1) were obtained in satisfactory yield. Compound **11** was instead obtained submitting the triazole **30** to direct acylation with benzoyl chloride in *N*,*N*-dimethylformamide (DMF) as the solvent (Scheme 1).

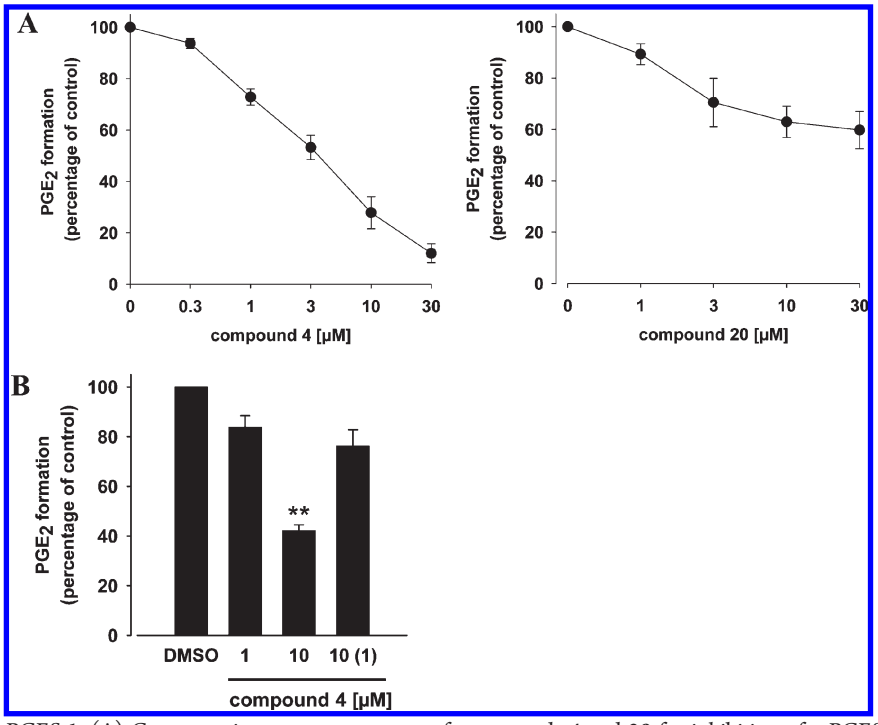

Figure 3. Inhibition of mPGES-1. (A) Concentration−response curves of compounds **4** and **20** for inhibition of mPGES-1 activity in microsomal preparations of IL-1β-stimulated A549 cells. (B) Reversibility of mPGES-1 inhibition by compound **4**. Wash-out experiments were performed as described in the text. Data are given as means ± SEs, $n = 4-5$; $^{**}p < 0.01$.

Finally, to synthesize compound **23**, we took advantage of a multicomponent one-pot reaction between phenyl-1-propyne **40** and azidomethyl phenyl sulfide **27** in the presence of CuI-NBS (*N*-bromosuccinimide) and diisopropylethylamine (DIPEA); this step provided the desired 1,4,5 trisubstitued-1,2,3-triazole **41** bearing an iodine atom at the C-5 position (Scheme 2).[46] In the last step, the triazole intermediate **41** was subjected to the Suzuki cross-coupling reaction with 4-formyl-phenyl-boronic acid **42**, affording compound **23** in good yield.

Before submitting the test compounds **4**, **6**−**8**, **14**, **15**, **17**, **18**, **20**−**24**, and **26** synthetically obtained to the biological assays, their purities (>95%) were verified by Agilent Technologies 1200 series high-performance liquid chromatography (HPLC) with ultraviolet (UV) detection at 280 nm (method: Jupiter C-18 column, 250 mm × 4.60 mm, 5 μm, 300 Å; 1.0 mL/min flow rate; 5−100% in 30 min of 0.1% TFA/CH_3CN−0.1% TFA/H_2O).

Analysis of the Bioactivity. To assess the ability of the selected compounds **4**, **6**−**8**, **11**, **14**, **15**, **17**, **18**, **20**−**24**, and **26** to interfere with the activity of mPGES-1, a cell-free assay using the microsomal fractions of interleukin-1β (IL-1β)-stimulated A549 cells (as source for mPGES-1) was applied. In a first screening round, all compounds, solubilized in dimethyl sulfoxide (DMSO), were tested at concentrations of 30 μM. Because of the limited solubility of the test compounds in aqueous assay buffers, concentrations >30 μM could not be tested. The mPGES-1 inhibitor compound **43** (IC_{50} = 2.4 μM)[47] was used as a reference control, and DMSO (0.3%, v/v) was used as a vehicle control. As shown in Table 2, compounds **4**, **7**, **20**, and **23** significantly inhibited mPGES-1 activity, whereas all other derivatives were not significantly active at a concentration of 30 μM. Interestingly, these data confirm the results from the docking studies favoring **4** and **20** as mPGES-1 inhibitors. More detailed analysis of **4** in concentration−response studies (Figure 3A) revealed an IC_{50} value of 3.2 μM and indicated an almost complete inhibition of mPGES-1 activity at 30 μM. In contrast to **4**, compound **20** failed to entirely suppress mPGES-1 activity, and the concentration−response curve seemingly reached a plateau with maximum inhibition of approximately 40% at the highest concentration (Figure 3A). Similarly, for compounds **7** and **23**, the maximal inhibition at 30 μM was less than 40%, and thus, IC_{50} could not be obtained. Wash-out experiments suggest a reversible mode of action of compound **4**, as 10-fold dilution of the incubation mixture reversed mPGES-1 inhibition by **4** (Figure 3B).

Previous studies on acidic mPGES-1 inhibitors showed that such compounds often interact also with other enzymes within the arachidonic acid cascade, such as 5-LO or FLAP. In fact, interference with 5-LO or FLAP, the key enzymes in the formation of leukotrienes (LTs) from arachidonic acid, is considered a valuable characteristic of a given mPGES-1 inhibitor, because dual suppression of PGE_2 and LT formation might be superior over single interference in terms of higher anti-inflammatory efficacy as well as in terms of reduced side effects.[48] Thus, we further analyzed the test compounds (30 μM, each) for inhibition of 5-LO activity in a cell-free assay using isolated human recombinant 5-LO as the enzyme source. The well-recognized 5-LO inhibitor (*E*)-*N*-hydroxy-*N*-(3-(3-phenoxyphenyl)-allyl)acetamide (BWA4C)[49] was used as a positive control, and DMSO (0.3%, v/v) was used as a vehicle control. Intriguingly, among the test compounds, **20** was the most active derivative with IC_{50} = 0.8 μM, followed by **21**, **4**, **17**, and **7** (Table 3, IC_{50} = 4.1, 6.7, 8.8, and 27 μM, respectively), which all inhibited 5-LO activity in a concentration-dependent manner (Figure 4A). 5-LO inhibition was reversible, as demonstrated by wash-out experiments (not shown). Also, **6**, **14**, **23**, and **26** significantly inhibited 5-LO at a concentration of 30 μM, but the

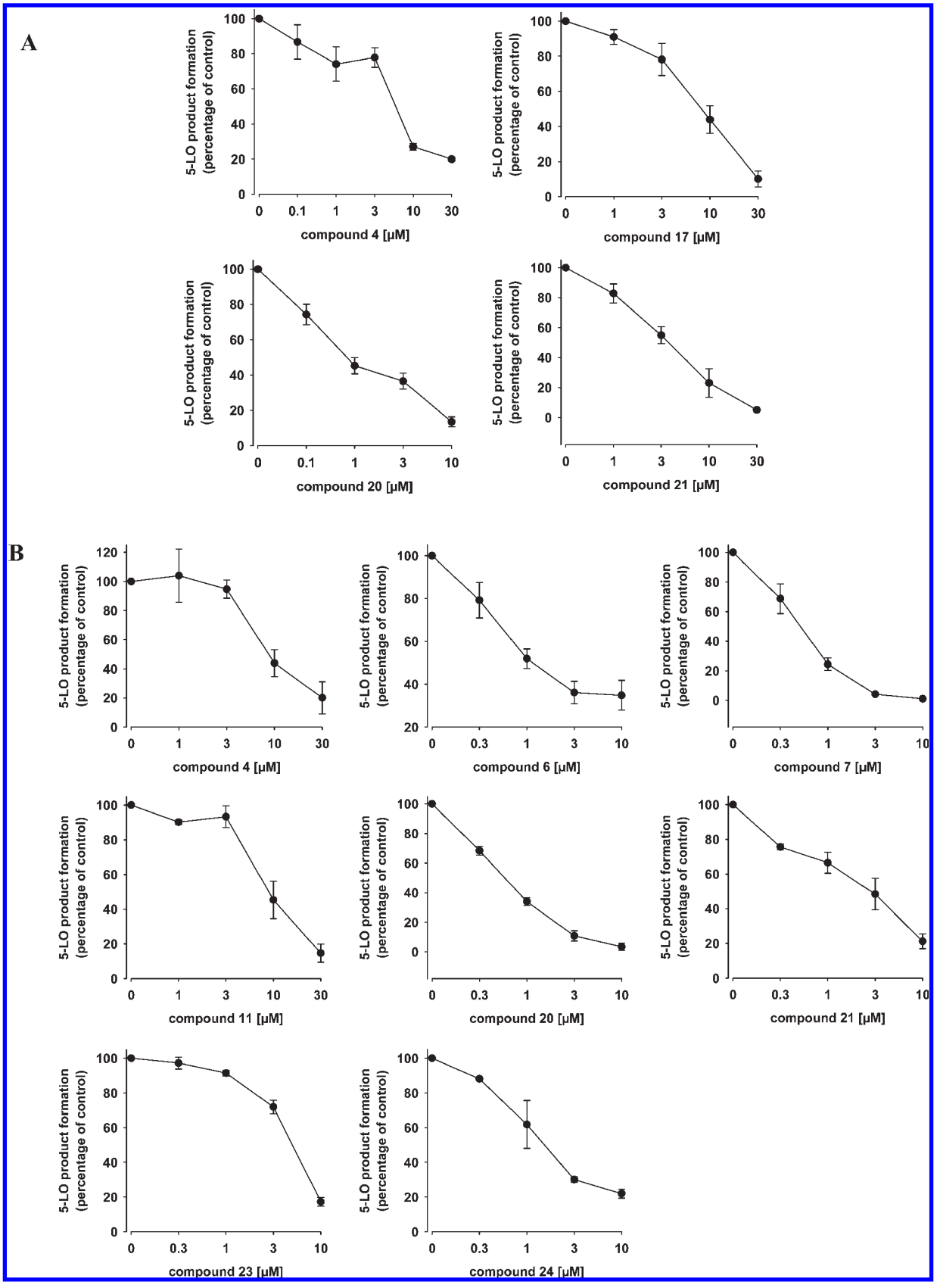

Figure 4. Inhibition of 5-LO. (A) Concentration−response studies for purified recombinant 5-LO. (B) Concentration−response studies for 5-LO product formation in intact human neutrophils. Data are given as means ± SEs, $n = 4-5$.

dx.doi.org/10.1021/jm101238d |*J. Med. Chem.* 2011, 54, 1565–1575

Table 3. Effect of Test Compounds on the Activity of 5-LO in Cell-Free and Cell-Based (Intact Neutrophils) Assays[a]

	5-LO activity; cell-free		5-LO activity; intact neutrophils	
compound	IC $_{50}$ (μM)	remaining activity at 30 μM (%)	IC $_{50}$ (μM)	remaining activity at 30 μM (%)
4	6.7	20.0 ± 0.9**	9.2	20.1 ± 11.0**
6	>30	62.3 ± 1.4**	0.9	34.8 ± 7.0**[b]
7	27	48.8 ± 0.4**	0.4	1.1 ± 0.3**[b]
8	>30	82.9 ± 0.9	>30	85.7 ± 3.5
11	>30	80.8 ± 5.3	9.3	14.6 ± 5.2**
14	>30	58.4 ± 12.7*	>30	70.2 ± 8.5
15	>30	77.4 ± 0.9	>30	79.9 ± 10.7
17	8.8	10.1 ± 4.6**	>30	52.7 ± 15.0*
18	>30	82.5 ± 4.4	>30	92.1 ± 8.1
20	0.8	13.6 ± 2.8**[b]	0.6	3.5 ± 2.5**[b]
21	4.1	5.1 ± 0.8**	2.8	21.2 ± 4.3**[b]
22	>30	78.4 ± 10.3	>30	84.5 ± 3.4
23	>30	57.3 ± 1.2**	6.0	17.3 ± 2.5**[b]
24	>30	60.7 ± 10.0	1.7	22.0 ± 2.6**[b]
26	>30	59.2 ± 6.4*	>30	70.1 ± 9.0

[a] Data are given as means ± SEs, n = 4−6. *p < 0.05, and **p < 0.01. [b] Remaining activity at 10 μM.

Chart 2. Chemical Structures of 43 and 44

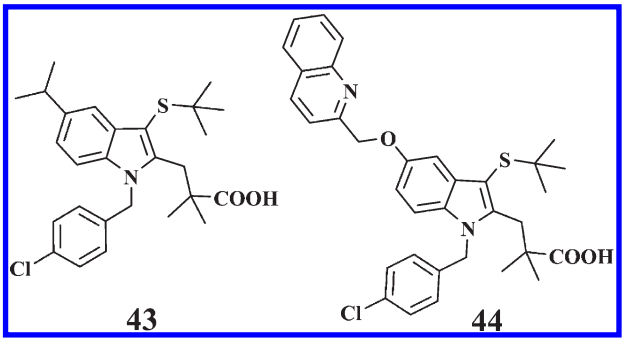

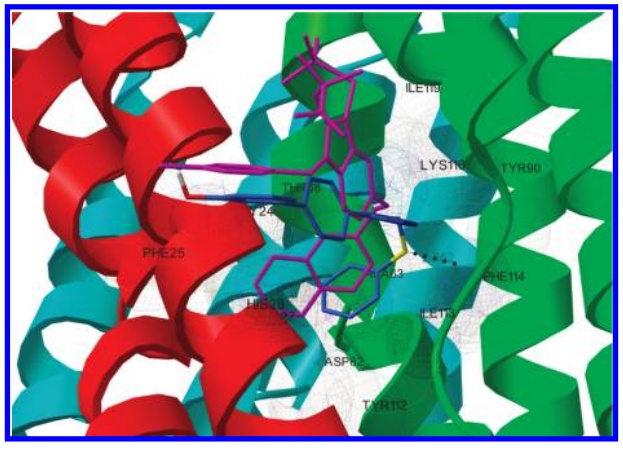

Figure 5. Three-dimensional model of interactions between **7** and FLAP. The protein is represented by secondary structure, by CPK, and by lines colored by atom type (by atom type: C, gray; polar H, sky blue; N, blue; O, red; and S, yellow). Compound **7** is depicted by sticks and balls (by atom type: C, sky blue; O, red; N, dark blue; S, yellow; and H, white). Compound **44** is depicted by sticks and balls (C, O, N, S, and Cl dark pink). The figure highlights similar interactions for both **7** and **44** with arachidonic acid-binding site.

magnitude of inhibition did not exceed 50% (Table 3), and thus, IC_{50} values could not be determined.

Because FLAP inhibitors do not inhibit 5-LO activity in cell-free assays but only LT formation in intact cells,[50] we assessed a potential inhibitory effect on FLAP in human neutrophils activated by ionophore A23187. Compound **43** (IC_{50} for FLAP in neutrophils approximately 70 nM)[51] served as the control, and DMSO (0.3%, v/v) was used as the vehicle control. Compounds **4**, **6**, **7**, **11**, **20**, **21**, **23**, and **24** reduced 5-LO product formation at 30 μM by more than 50% in a concentration-related manner with IC_{50} values in the range of 0.4−9.3 μM (Table 3 and Figure 4B). For **4** and **20**, the IC_{50} values were determined at 8.8 and 0.6 μM, respectively, which fits well with the activities in cell-free 5-LO assays, and also, **21** was similarly efficient (IC_{50} = 2.8 μM) as for isolated 5-LO.

A remarkable and concentration-dependent suppression of cellular 5-LO product synthesis was found for **7** with IC_{50} = 0.4 μM and also for **6** and **24** (IC_{50} = 0.9 and 1.7 μM, respectively), although these compounds hardly inhibited 5-LO in the cell-free assay. This suggests that for suppression of 5-LO product formation in intact cells, **6**, **7**, and **24** may primarily act at other targets than the 5-LO enzyme, presumably on FLAP. Such mechanisms may also be attributed to compounds **11** and **23**, although with lower potencies (IC_{50} = 9.3 and 6 μM, respectively).

All in all, on the basis of the outcomes of the biological activity data, **4** is the most efficient inhibitor of mPGES-1, **7** might act as a FLAP inhibitor, while **20** might be a potent direct 5-LO inhibitor, besides moderate inhibition of mPGES-1. Hence, we aimed to rationalize the results through molecular modeling studies. As preliminarily remarked, it should be put in evidence that compounds **4** and **7**, inhibiting the two MAPEG family members, showed quite similar chemical features; on the contrary, the more encumbering ligand **20** seems to target no structurally related MAPEG enzymes. For our calculations, we used the 3D structure of FLAP in complex with the inhibitor **44** (MK-591, Chart 2)[52] solved by Ferguson et al.[53] in 2007 [protein data bank (PDB) ID code 2Q7M]. Because of the lack of crystal structure information on 5-LO, we used a 15-LO[54] (PDB ID code 1LOX) enzyme,

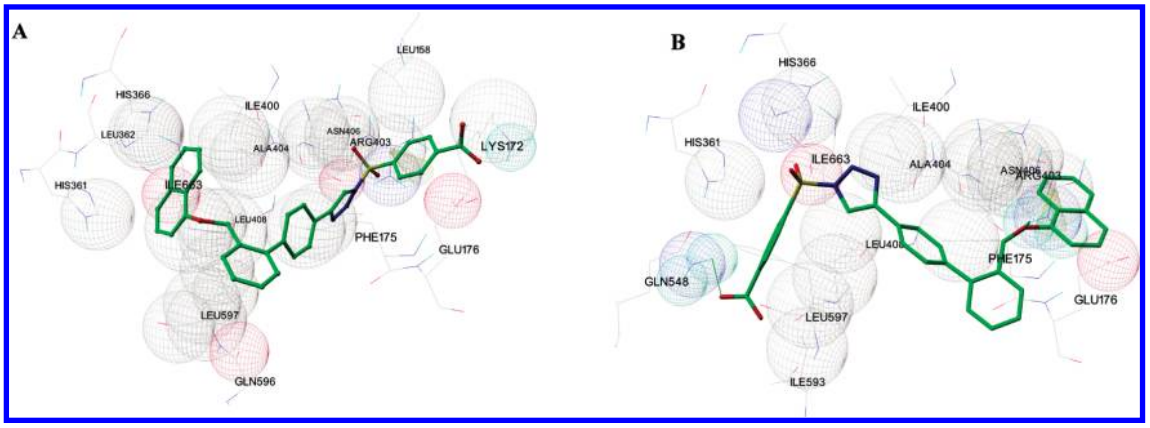

Figure 6. Three-dimensional model of interactions of **20** and 15-lipoxygenase enzyme active site. The protein is represented by CPK and by lines colored by atom type (by atom type: C, gray; polar H, sky blue; N, blue; O, red; and S, yellow). Two different conformations (A and B) of the complex are depicted. Compound **20** is depicted by sticks and balls (by atom type: C, green; O, red; N, dark blue; and S, yellow).

presenting the highest sequence similarity (38% identity with human 5-LO; see the Supporting Information) among the dioxygenase family (8-, 9-, 11-, and 12-LO).

Taking into account the considerations reported above for the MGST-1 enzyme, also in the case of FLAP, the binding specificity was conferred by the H-bond with the Lys116. In our proposed pose, **7** (Figure 5) not only interacts with the fundamental amino acids but also adopts the equivalent spatial disposition of the cocrystallized inhibitor,[54] maintaining the same interactions network. Moreover, the phenyl group in R_1 forms a $\pi-\pi$ stacking with Phe25.

Three different classes of inhibitors can be generally considered for 5-LO:[55] (1) antioxidant agents interfering with the redox catalytic cycle of the enzyme, (2) iron-chelating agents, and (3) nonredox type inhibitors, which compete with arachidonic acid for the binding to the enzyme.[50] In our docking studies, we supposed that **20** acts as nonredox type LO inhibitor. As described for mPGES-1, the rationalization of the 5-LO binding mode was obtained considering the fundamental amino acids in the active site of the enzyme as reported by Charlier et al.[56] (see the Supporting Information), taking into consideration the specific polar interaction of the carboxylate moiety of arachidonic acid with $Lys409_{5\text{-}L0}$ ($Arg403_{15\text{-}LO}$).

For compound **20**, we obtained two different conformation families, accounting for two independent high affinity binding modes (Figure 6A,B). In both of the conformations, the specific interaction with Arg403 was maintained. In particular, in the first conformation (Figure 6A), the phenyl group in R_1 shows a cation$-\pi$ interaction, while in the second conformation (Figure 6B), the same cation$-\pi$ interaction with Arg403 was exerted by the naphtyl group in R_2 present in the alternative conformation. In the latter case, the oxygen atom in R_2 forms an additional H-bond with the positively charged (Arg403) residue. Even if R_1 and R_2 are located on the opposite sites of the target pocket, and the other interactions with the receptor counterpart remain unmodified and are in accordance with the structural requirements indicated by Charlier et al.,[56] that is, two hydrophobic groups, an aromatic ring, and two hydrogen bond acceptors.

CONCLUSIONS

We have applied a rapid in silico screening on a small set of triazole derivates for directing the click chemistry synthesis of the most promising mPGES-1 inhibitor **4**. In light of the good qualitative accordance between the results from the biological assays and the prediction of the molecular docking calculations, a satisfactory explanation of the putative binding mode for the new triazole based compounds was provided. Biological assays disclosed three different benchmark compounds **4**, **7**, and **20** as inhibitors of mPGES-1, FLAP, and 5-LO, respectively. The future perspectives, in fact, regard the decoration of the triazole ring with more polar in nature R_1 and R_2, in order to increase their solubility in the biological liquids. At the moment, the most feasible improvement for the development of new mPGES-1 inhibitors consists of generating analogues of **4** with a R_2-modified position. In particular, the fundamental biphenyl portion—present in the three different compounds **4**, **7**, and **20**—needs a more appropriate substitution pattern to increase the interaction efficiency with the polar aminoacids of the catalytic site (e.g., Thr33, Arg37, Lys67, and Arg129). In conclusion, our results prove the efficiency of the triazole group as a new scaffold useful in the rational design of new promising candidates as anti-inflammatory drugs and shed light on the chemical decorations functional for the design of further members belonging to this new class of inhibitors.

ASSOCIATED CONTENT

Supporting Information. Docking calculations and their detailed results; detailed procedure for the synthesis of compounds **4**, **6**−**8**, **11**, **14**, **15**, **17**, **18**, **20**−**24**, and **26**; HPLC conditions and nuclear magnetic resonance (NMR) data for the tested compounds; and protocol of the bioactivity assays. This material is available free of charge via the Internet at http://pubs.acs.org.

AUTHOR INFORMATION

Corresponding Author

*(I.B.) Tel: +39 089 969743. Fax: +39 089 969602. E-mail: brunoin@unisa.it. (G.B.) Tel: +39 089 969741. Fax: +39 089 969602. E-mail: bifulco@unisa.it.

ACKNOWLEDGMENT

Financial support by the University of Salerno and by Ministero dell'Istruzione, dell'Università e della Ricerca (MIUR),

PRIN-06, and Aureliasan GmbH (Tuebingen, Germany) is gratefully acknowledged.

■ ABBREVIATIONS USED

GSH, tripeptide glutathione; MAPEG, membrane-associated proteins in eicosanoid and glutathione metabolism; MGST-1, microsomal glutathione transferase 1; mPGES-1, microsomal prostaglandin E_2 synthase; 5-LO, 5-lipoxygenase; FLAP, 5-lipoxygenase-activating protein; COX, cyclooxygenase; PG, prostaglandin; LT, leukotriene; LTCS, leukotrien C synthase; IL-1β, interleukin 1β; PDB, protein data bank; NSAID, nonsteroidal anti-inflammatory drug; QM, quantum mechanic; SAR, structure−activity relationship; QSAR, quantitative structure−activity relationship; HTS, high-throughput screening; DMF, dimethylformamide; THF, tetrahydrofuran; DIPEA, *N*,*N*-diisopropylethylamine; DMSO, dimethylsulfoxide; NBS, *N*-bromosuccinimide

■ REFERENCES

(1) Funk, C. D. Prostaglandins and leukotrienes: Advances in eicosanoid biology. *Science* **2001**, *294*, 1871–1875.

(2) Wang, D.; Dubois, R. N. Prostaglandins and cancer. *Gut* **2006**, *55*, 115–122.

(3) Buttgereit, F.; Burmester, G. R.; Simon, L. S. Gastrointestinal toxic side effects of nonsteroidal anti-inflammatory drugs and cyclooxygenase-2-specific inhibitors. *Am. J. Med.* **2001**, *110* (Suppl. 3A), 13S–19S.

(4) McGettigan, P.; Henry, D. Cardiovascular risk and inhibition of cyclooxygenase: a systematic review of the observational studies of selective and nonselective inhibitors of cyclooxygenase 2. *J. Am. Med. Assoc.* **2006**, *296*, 1633–1644.

(5) Claveau, D.; Sirinyan, M.; Guay, J.; Gordon, R.; Chan, C. C.; Bureau, Y.; Riendeau, D.; Mancini, J. A. Microsomal prostaglandin E synthase-1 is a major terminal synthase that is selectively up-regulated during cyclooxygenase-2-dependent prostaglandin E2 production in the rat adjuvant-induced arthritis model. *J. Immunol.* **2003**, *170*, 4738–4744.

(6) Yoshimatsu, K.; Golijanin, D.; Paty, P. B.; Soslow, R. A.; Jakobsson, P. J.; DeLellis, R. A.; Subbaramaiah, K.; Dannenberg, A. J. Inducible microsomal prostaglandin E synthase is overexpressed in colorectal adenomas and cancer. *Clin. Cancer Res.* **2001**, *7*, 3971–3976.

(7) Yoshimatsu, K.; Altorki, N. K.; Golijanin, D.; Zhang, F.; Jakobsson, P. J.; Dannenberg, A. J.; Subbaramaiah, K. Inducible prostaglandin E synthase is overexpressed in non-small cell lung cancer. *Clin. Cancer Res.* **2001**, *7*, 2669–2674.

(8) Mehrotra, S.; Morimiya, A.; Agarwal, B.; Konger, R.; Badve, S. Microsomal prostaglandin E2 synthase-1 in breast cancer: A potential target for therapy. *J. Pathol.* **2006**, *208*, 356–363.

(9) Jakobsson, P. J.; Thoren, S.; Morgenstern, R.; Samuelsson, B. Identification of human prostaglandin E synthase: A microsomal, glutathione-dependent, inducible enzyme, constituting a potential novel drug target. *Proc. Natl. Acad. Sci. U.S.A.* **1999**, *96*, 7220–7225.

(10) Friesen, R. W.; Mancini, J. A. Microsomal prostaglandin E2 synthase-1 (mPGES-1): A novel anti-inflammatory therapeutic target. *J. Med. Chem.* **2008**, *51*, 4059–4067.

(11) Murakami, M.; Naraba, H.; Tanioka, T.; Semmyo, N.; Nakatani, Y.; Kojima, F.; Ikeda, T.; Fueki, M.; Ueno, A.; Oh, S.; Kudo, I. Regulation of prostaglandin E2 biosynthesis by inducible membrane-associated prostaglandin E2 synthase that acts in concert with cyclooxygenase-2. *J. Biol. Chem.* **2000**, *275*, 32783–32792.

(12) Jegerschold, C.; Pawelzik, S. C.; Purhonen, P.; Bhakat, P.; Gheorghe, K. R.; Gyobu, N.; Mitsuoka, K.; Morgenstern, R.; Jakobsson, P. J.; Hebert, H. Structural basis for induced formation of the inflammatory mediator prostaglandin E2. *Proc. Natl. Acad. Sci. U.S.A.* **2008**, *105*, 11110–11115.

(13) Congreve, M.; Chessari, G.; Tisi, D.; Woodhead, A. J. Recent developments in fragment-based drug discovery. *J. Med. Chem.* **2008**, *51*, 3661–3680.

(14) Shelke, S. V.; Cutting, B.; Jiang, X.; Koliwer-Brandl, H.; Strasser, D. S.; Schwardt, O.; Kelm, S.; Ernst, B. A fragment-based in situ combinatorial approach to identify high-affinity ligands for unknown binding sites. *Angew. Chem., Int. Ed. Engl.* **2010**, *49*, 5721–5725.

(15) Nestler, H. P. Combinatorial chemistry and fragment screening—Two unlike siblings? *Curr. Drug Discovery Technol.* **2005**, *2*, 1–12.

(16) Mamidyala, S. K.; Finn, M. G. In situ click chemistry: Probing the binding landscapes of biological molecules. *Chem. Soc. Rev.* **2010**, *39*, 1252–1261.

(17) Moses, J. E.; Moorhouse, A. D. The growing applications of click chemistry. *Chem. Soc. Rev.* **2007**, *36*, 1249–1262.

(18) Rees, D. C.; Congreve, M.; Murray, C. W.; Carr, R. Fragment-based lead discovery. *Nat. Rev. Drug Discovery* **2004**, *3*, 660–672.

(19) Kolb, H. C.; Sharpless, K. B. The growing impact of click chemistry on drug discovery. *Drug Discovery Today* **2003**, *8*, 1128–1137.

(20) Pasha, F. A.; Muddassan, M.; Jung, H.; Yang, B. S.; Lee, C.; Soo Oh, J.; Joo Cho, S.; Cho, H. QM and pharmacophore based 3D-QSAR of MK886 analogues against mPGES-1. *Bull. Korean Chem.* **2008**, *29*, 647–655.

(21) Giroux, A.; Boulet, L.; Brideau, C.; Chau, A.; Claveau, D.; Cote, B.; Ethier, D.; Frenette, R.; Gagnon, M.; Guay, J.; Guiral, S.; Mancini, J.; Martins, E.; Masse, F.; Methot, N.; Riendeau, D.; Rubin, J.; Xu, D.; Yu, H.; Ducharme, Y.; Friesen, R. W. Discovery of disubstituted phenanthrene imidazoles as potent, selective and orally active mPGES-1 inhibitors. *Bioorg. Med. Chem. Lett.* **2009**, *19*, 5837–5841.

(22) Wang, J.; Limburg, D.; Carter, J.; Mbalaviele, G.; Gierse, J.; Vazquez, M. Selective inducible microsomal prostaglandin E(2) synthase-1 (mPGES-1) inhibitors derived from an oxicam template. *Bioorg. Med. Chem. Lett.* **2010**, *20*, 1604–1609.

(23) San Juan, A. A.; Cho, S. J. 3D-QSAR study of microsomal prostaglandin E2 synthase (mPGES-1) inhibitors. *J. Mol. Model.* **2007**, *13*, 601–610.

(24) AbdulHameed, M. D.; Hamza, A.; Liu, J.; Huang, X.; Zhan, C. G. Human microsomal prostaglandin E synthase-1 (mPGES-1) binding with inhibitors and the quantitative structure-activity correlation. *J. Chem. Inf. Model.* **2008**, *48*, 179–185.

(25) San Juan, A. A.; Cho, S. J.; Cho, H. HQSAR study of microsomal prostaglandin E_2 synthase (mPGES-1) inhibitors. *Bull. Korean Chem. Soc.* **2006**, *27*, 1531–1536.

(26) Calvin, Y. A. A. Pharmacoinformatics approach for mPGES-1 in anti-inflammation by 3D-QSAR pharmacophore mapping. *J. Taiwan Inst. Chem.* **2009**, *40*, 155–161.

(27) Rorsch, F.; Wobst, I.; Zettl, H.; Schubert-Zsilavecz, M.; Grosch, S.; Geisslinger, G.; Schneider, G.; Proschak, E. Nonacidic inhibitors of human microsomal prostaglandin synthase 1 (mPGES 1) identified by a multistep virtual screening protocol. *J. Med. Chem.* **2010**, *53*, 911–915.

(28) Cote, B.; Boulet, L.; Brideau, C.; Claveau, D.; Ethier, D.; Frenette, R.; Gagnon, M.; Giroux, A.; Guay, J.; Guiral, S.; Mancini, J.; Martins, E.; Masse, F.; Methot, N.; Riendeau, D.; Rubin, J.; Xu, D.; Yu, H.; Ducharme, Y.; Friesen, R. W. Substituted phenanthrene imidazoles as potent, selective, and orally active mPGES-1 inhibitors. *Bioorg. Med. Chem. Lett.* **2007**, *17*, 6816–6820.

(29) Hamza, A.; AbdulHameed, M. D.; Zhan, C. G. Understanding microscopic binding of human microsomal prostaglandin E synthase-1 with substrates and inhibitors by molecular modeling and dynamics simulation. *J. Phys. Chem. B* **2008**, *112*, 7320–7329.

(30) Hamza, A.; Tong, M.; AbdulHameed, M. D. M.; Liu, J.; Goren, A. C.; Tai, H. H.; Zhan, C. G. Understanding microscopic binding of human microsomal prostaglandin E synthase-1 (mPGES-1) trimer with substrate PGH_2 and cofactor GSH: insights from computational alanine scanning and site-directed mutagenesis. *J. Phys. Chem.* **2010**, *114*, 5605–5616.

(31) Quraishi, O.; Mancini, J. A.; Riendeau, D. Inhibition of inducible prostaglandin E(2) synthase by 15-deoxy-Delta(12,14)-prostaglandin

J(2) and polyunsaturated fatty acids. *Biochem. Pharmacol.* **2002**, *63*, 1183–1189.

(32) Riendeau, D.; Aspiotis, R.; Ethier, D.; Gareau, Y.; Grimm, E. L.; Guay, J.; Guiral, S.; Juteau, H.; Mancini, J. A.; Methot, N.; Rubin, J.; Friesen, R. W. Inhibitors of the inducible microsomal prostaglandin E2 synthase (mPGES-1) derived from MK-886. *Bioorg. Med. Chem. Lett.* **2005**, *15*, 3352–3355.

(33) Morris, G. M.; Goodsell, D. S.; Halliday, R. S.; Huey, R.; Hart, W. E.; Belew, R. K.; Olson, A. J. Automated docking using a lamarckian genetic algorithm and an empirical binding free energy function. *J. Comput. Chem.* **1998**, *19*, 1662.

(34) Holm, P. J.; Bhakat, P.; Jegerschold, C.; Gyobu, N.; Mitsuoka, K.; Fujiyoshi, Y.; Morgenstern, R.; Hebert, H. Structural basis for detoxification and oxidative stress protection in membranes. *J. Mol. Biol.* **2006**, *360*, 934–945.

(35) Thoren, S.; Weinander, R.; Saha, S.; Jegerschold, C.; Pettersson, P. L.; Samuelsson, B.; Hebert, H.; Hamberg, M.; Morgenstern, R.; Jakobsson, P. J. Human microsomal prostaglandin E synthase-1: Purification, functional characterization, and projection structure determination. *J. Biol. Chem.* **2003**, *278*, 22199–22209.

(36) Kuntz, I. D.; Chen, K.; Sharp, K. A.; Kollman, P. A. The maximal affinity of ligands. *Proc. Natl. Acad. Sci. U.S.A.* **1999**, *96*, 9997–10002.

(37) Abad-Zapatero, C.; Metz, J. T. Ligand efficiency indices as guideposts for drug discovery. *Drug Discovery Today* **2005**, *10*, 464–469.

(38) Hetenyi, C.; Maran, U.; Garcia-Sosa, A. T.; Karelson, M. Structure-based calculation of drug efficiency indices. *Bioinformatics* **2007**, *23*, 2678–2685.

(39) Wells, J. A.; McClendon, C. L. Reaching for high-hanging fruit in drug discovery at protein-protein interfaces. *Nature* **2007**, *450*, 1001–1009.

(40) Rostovtsev, V. V.; Green, L. G.; Fokin, V. V.; Sharpless, K. B. A stepwise huisgen cycloaddition process: Copper(I)-catalyzed regioselective "ligation" of azides and terminal alkynes. *Angew. Chem., Int. Ed. Engl.* **2002**, *41*, 2596–2599.

(41) Appukkuttan, P.; Dehaen, W.; Fokin, V. V.; Van der, E. E. A microwave-assisted click chemistry synthesis of 1,4-disubstituted 1,2,3-triazoles via a copper(I)-catalyzed three-component reaction. *Org. Lett.* **2004**, *6*, 4223–4225.

(42) Whiting, M.; Fokin, V. V. Copper-catalyzed reaction cascade: direct conversion of alkynes into N-sulfonylazetidin-2-imines. *Angew. Chem., Int. Ed. Engl.* **2006**, *45*, 3157–3161.

(43) Cassidy, M. P.; Raushel, J.; Fokin, V. V. Practical synthesis of amides from in situ generated copper(I) acetylides and sulfonyl azides. *Angew. Chem., Int. Ed. Engl.* **2006**, *45*, 3154–3157.

(44) Yoo, E. J.; Ahlquist, M.; Kim, S. H.; Bae, I.; Fokin, V. V.; Sharpless, K. B.; Chang, S. Copper-catalyzed synthesis of N-sulfonyl-1,2,3-triazoles: Controlling selectivity. *Angew. Chem., Int. Ed. Engl.* **2007**, *46*, 1730–1733.

(45) Aquino, M.; Guerrero, M. D.; Bruno, I.; Terencio, M. C.; Paya, M.; Riccio, R. Development of a second generation of inhibitors of microsomal prostaglandin E synthase 1 expression bearing the gamma-hydroxybutenolide scaffold. *Bioorg. Med. Chem.* **2008**, *16*, 9056–9064.

(46) Li, L.; Zhang, G.; Zhu, A.; Zhang, L. A convenient preparation of 5-iodo-1,4-disubstituted-1,2,3-triazole: Multicomponent one-pot reaction of azide and alkyne mediated by CuI-NBS. *J. Org. Chem.* **2008**, *73*, 3630–3633.

(47) Koeberle, A.; Siemoneit, U.; Buhring, U.; Northoff, H.; Laufer, S.; Albrecht, W.; Werz, O. Licofelone suppresses prostaglandin E2 formation by interference with the inducible microsomal prostaglandin E2 synthase-1. *J. Pharmacol. Exp. Ther.* **2008**, *326*, 975–982.

(48) Koeberle, A.; Werz, O. Inhibitors of the microsomal prostaglandin E(2) synthase-1 as alternative to non steroidal anti-inflammatory drugs (NSAIDs)—A critical review. *Curr. Med. Chem.* **2009**, *16*, 4274–4296.

(49) Tateson, J. E.; Randall, R. W.; Reynolds, C. H.; Jackson, W. P.; Bhattacherjee, P.; Salmon, J. A.; Garland, L. G. Selective inhibition of arachidonate 5-lipoxygenase by novel acetohydroxamic acids: biochemical assessment in vitro and ex vivo. *Br. J. Pharmacol.* **1988**, *94*, 528–539.

(50) Werz, O. 5-Lipoxygenase: Cellular biology and molecular pharmacology. *Curr. Drug Targets Inflamm. Allergy* **2002**, *1*, 23–44.

(51) Fischer, L.; Hornig, M.; Pergola, C.; Meindl, N.; Franke, L.; Tanrikulu, Y.; Dodt, G.; Schneider, G.; Steinhilber, D.; Werz, O. The molecular mechanism of the inhibition by licofelone of the biosynthesis of 5-lipoxygenase products. *Br. J. Pharmacol.* **2007**, *152*, 471–480.

(52) Mendis, C.; Campbell, K.; Das, R.; Yang, D.; Jett, M. Effect of 5-lipoxygenase inhibitor MK591 on early molecular and signaling events induced by staphylococcal enterotoxin B in human peripheral blood mononuclear cells. *FEBS J.* **2008**, *275*, 3088–3098.

(53) Ferguson, A. D.; McKeever, B. M.; Xu, S.; Wisniewski, D.; Miller, D. K.; Yamin, T. T.; Spencer, R. H.; Chu, L.; Ujjainwalla, F.; Cunningham, B. R.; Evans, J. F.; Becker, J. W. Crystal structure of inhibitor-bound human 5-lipoxygenase-activating protein. *Science* **2007**, *317*, 510–512.

(54) Gillmor, S. A.; Villasenor, A.; Fletterick, R.; Sigal, E.; Browner, M. F. The structure of mammalian 15-lipoxygenase reveals similarity to the lipases and the determinants of substrate specificity. *Nat. Struct. Biol.* **1997**, *4*, 1003–1009.

(55) Werz, O. Inflammation and allergy. *Curr. Drug Targets* **2002**, *1*, 23–44.

(56) Charlier, C.; Henichart, J. P.; Durant, F.; Wouters, J. Structural insights into human 5-lipoxygenase inhibition: Combined ligand-based and target-based approach. *J. Med. Chem.* **2006**, *49*, 186–195.